Tetrahedron 67 (2011) 4814–4819

Contents lists available at ScienceDirect

Tetrahedron

journal homepage: www.elsevier.com/locate/tet

Steric effects on controlling of photoinduced electron transfer action of anthracene modified benzo-15-crown-5 by complexation with Mg^{2+} and Ca^{2+}

Jeongsik Kim [a,b], Yoshikazu Oka [b], Tatsuya Morozumi [c], Eun Wha Choi [d], Hiroshi Nakamura [c,*]

[a] Advanced Materials Division, Korea Research Institute of Chemical Technology, Daejeon 305-606, South Korea
[b] Division of Environmental Earth Science, Graduate School of Environmental Science, Hokkaido University, Sapporo, Hokkaido 060-0810, Japan
[c] Research Faculty of Environmental Earth Science, Hokkaido University, Sapporo, Hokkaido 060-0810, Japan
[d] Drug Discovery Division, Korea Research Institute of Chemical Technology, Daejeon 305-606, South Korea

ARTICLE INFO

Article history:
Received 25 November 2010
Received in revised form 9 May 2011
Accepted 9 May 2011
Available online 14 May 2011

Keywords:
Photoinduced electron transfer
Anthracene
Steric effect
Chemosensor
Benzo-15-crown-5

ABSTRACT

Benzo-crown ether based chemosensors linked by an amide bond at the 1-, 2- or 9-positions of anthracene rings were synthesized. Their complexation behavior with alkaline earth metal ions in acetonitrile was investigated using fluorescence, UV, and ^{1}H NMR spectroscopy. In the absence of a metal ion, all compounds showed only very slight fluorescence emissions (fluorescence 'off' state) because of intramolecular charge/electron transfer process. After the complex formation with Mg^{2+} and Ca^{2+}, however, only the 2-position analogue gave a fluorescence 'on' response by inhibiting the photoinduced electron transfer. Because 2-positioned anthracene was free from steric hindrance of the crown ether ring, a strongly bent complex structure was formed with Mg^{2+} and Ca^{2+}, which induced a breakdown of π-conjugation between the amide moiety and the benzene ring.

1. Introduction

Crown ether based chemosensors with fluorescent detecting moieties have attracted considerable attention for their application as a chemical sensor for metal cations, anions, and molecules.[1] Most concepts developed to date are based mainly on photoinduced electron transfer (PET)[2] and intramolecular charge transfer (ICT)[3] systems for a signal transducer from the complex information. These PET sensors generally comprise a guest binding site as the receptor and fluorophore moiety, which causes changes of the fluorescence intensity and spectrum shape upon complexation with a guest molecule. For analytical studies for metal ion, the chemical sensor should be designed by the dependence on the chemical characteristics affected by a charge, coordination number, ionic radius, hardness, electronic potential etc.[4] If complexation behavior could be controlled by external inputs, such as light,[5] pH,[6] temperature,[7] and redox potential,[8] then it would present advantageous properties for analytical use. Among them, pH control would be easy; the PET process is linked strongly by pH and the coordination guest molecule. Therefore, such PET probes have emphasized the harmonious combination of cation receptor and selection of a suitable fluorophore.

In these contexts, we have already reported a series of new type fluorophores and their applications to construction of 'off–on' fluorescent sensing systems. These fluorescent moieties consist of popular fluorescent hydrocarbons and a benzene ring connected by an amide bond. They show fluorescent quenching through ICT from the benzene to the vacant HOMOs of fluorogenic hydrocarbons at the excited state. This ICT exhibited dramatic changes by the difference of substituted positions of electrodonating groups on the benzene ring. The ICT actions were categorized clearly into two groups by the introduction of electrodonating groups to *ortho*-positions or *para*-positions.[9] The ICT step of the *ortho* substitution group was involved in molecular geometry changes, such as twisted motion (twisted intramolecular charge transfer: TICT). In contrast, the ICT process of *para* substituted compounds requires no molecular motions as PET does. The former, the TICT process, can be controlled by inhibiting the twisted motion through a steric hindrance accompanying with complexation with guest molecules.[10] Several TICT chemosensors based on non-cyclic polyethers[11] and cyclodextrin[12] were developed. The latter, PET control was achieved by the employment of benzo-crown ether. Fluorescence intensity change was derived by breakdown of π–π interaction between fluorescent moieties and benzene rings upon complexation with alkaline earth metal ions. A series of benzo-crown ether bearing naphthalene,[13a] fluorene,[13b] and phenanthrene[13c] linked by amide bond have been synthesized, and their chemosensing characters were investigated.

* Corresponding author. E-mail address: nakamura@ees.hokudai.ac.jp (H. Nakamura).

0040-4020/$ – see front matter © 2011 Elsevier Ltd. All rights reserved.
doi:10.1016/j.tet.2011.05.042

In a previous report,[9] the authors synthesized a new fluorogenic benzo-crown ether having 9-anthracene (**9AC**) connected by the amide bond. Contrary to expectations, **9AC** showed no spectral change after the addition of guest ions, indicating that the breakdown of π–π conjugation upon complexation was insufficient to inhibit the PET process. This reason is explainable as follows: because **9AC** bound guest ions with crown ether and the carbonyl groups, the whole molecule was bent. A large steric repulsion between the crown ether fragment and the anthracene ring should arise. The steric repulsion presumably caused a shortage of the π–π conjugation breakdown. To cancel the steric crowdedness, it occurred to us that substituted position effects of anthracene ring were used. Introduction of benzo-crown ether to 1- and/or 2-position of the anthracene rings present sufficient steric margins and permitted sufficient bent complex structure.

With these in mind, we synthesized fluorescent benzo-15-crown-5s, **1AC** and **2AC**, as analogues to the non-fluorescent **9AC** (Scheme 1). No report in the relevant literature describes crown ether compound derivatives that can regulate their fluorescence state by substituted anthracene (9-, 1- or 2-substitution) as a monofluorophore. We herein report a crown ether type of chemical sensor that shows a distinct fluorescent 'off–on' response.

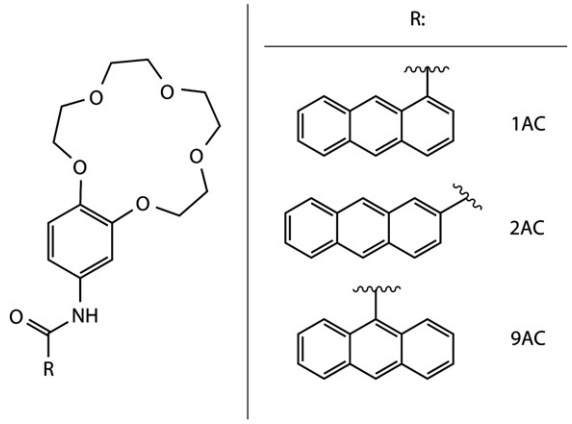

Scheme 1.

2. Results and discussion

2.1. Fluorescence spectra of 9AC, 1AC, and 2AC and their Mg^{2+} complexes

Fig. 1 presents fluorescence spectra of (a) **9AC**, (b) **1AC**, and (c) **2AC** as a function of the concentration of Mg^{2+} in acetonitrile at 25 °C. Fluorescence intensities of these free modified crown ethers were quite weak in the absence of cation. The relative fluorescence quantum yield (Φ_f) of free **2AC** was estimated to be 0.00039. The weak emission of free three crown ethers is probably attributable to the photoinduced electron transfer (PET) action from a crown ether fragment to the vacant HOMO of excited anthracene. The addition of Mg^{2+} did not induce enhancement of the fluorescence intensity of **1AC**, similarly to **9AC** reported previously.[9] The fluorescence emissions of **1AC** and **9AC** were not increased by the addition of any alkaline earth metal ion. These results suggest that the coordination of cations on the benzo-crown ether moiety and the carbonyl group connected to 9- and 1-anthracene ring was insufficient to break the PET pathway. In contrast, the fluorescence intensity increase of **2AC** with the addition of Mg^{2+} was observed at around 435 nm. The fluorescence emission of **2AC** indicated that the quenching relaxation process from benzo-crown ether moiety to anthracene ring would be generated via or beyond the amide bond. A similar fluorescence enhancement effect by the addition of Ca^{2+} was also obtained. The fluorescence response ratios of **2AC**, expressed as I_{max}/I_0 values for metal cations, are presented in Table 1. The order of I_{max}/I_0 was Mg^{2+} (29) ≈ Ca^{2+} (30) > Sr^{2+} (13) > Ba^{2+} (8.6). The **2AC** showed large quenching control ability for Mg^{2+} and Ca^{2+} compared to that of other metal cations. Φ_f of **2AC** with Ca^{2+} was also enhanced to 16-folds (Φ_f=0.0063). The binding constant (log *K*) of the complex was also evaluated from the fluorescence intensities using a nonlinear least-squares curve fitting method.[14] Among the alkaline earth cations, Mg^{2+} and Ca^{2+} showed the best affinity to **2AC**.

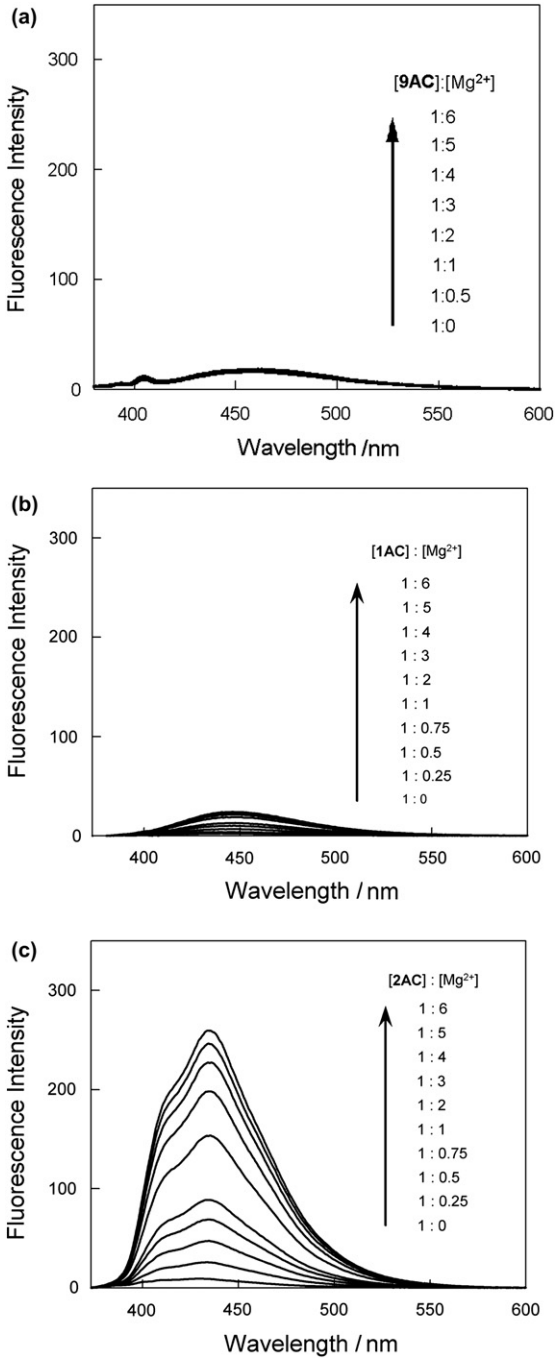

Fig. 1. Fluorescence spectra of (a) **9AC**, (b) **1AC**, (c) **2AC** and their Mg^{2+} complexes at 25 °C [**L**]=1×10^{-5} mol/dm^3, [Mg^{2+}]=(0, 0.25, 0.5, 0.75, 1, 2, 3, 4, 5, 6)$\times10^{-5}$ mol/dm^3.

Table 1
Fluorescence intensity ratios (I_{max}/I_0) of **2AC** at λ_{max}=435 nm and complex formation constants (log K)[a]

	Mg^{2+}	Ca^{2+}	Sr^{2+}	Ba^{2+}
I_{max}/I_0	29	30[b]	13	8.6
log K	5.32	5.24	4.48	4.54

[a] K=[complex]/([ligand] [metal ion]). Standard deviation is estimated to be 0.08.
[b] Obtained relative fluorescence quantum yields (Φ_f) were 0.00039 and 0.0063 in the absence and presence of Ca^{2+}.

Table 2
Chemical shifts [δ ppm] for **2AC** and **1AC** and chemical shift changes [$\Delta\delta$ ppm] and their complex with excess quantity of Mg^{2+} and Ca^{2+}. Numbers of hydrogens correspond to respective peaks in Fig. 2. $\Delta\delta$ values show lower field shifts

	2AC				**1AC**			
	11	12	13	14	11	12	13	14
None	8.84	7.27	6.95	7.53	8.75	7.26	6.98	7.53
Mg^{2+}	0.35	0.22	0.26	0.31	0.25	0.15	0.23	0.40
Ca^{2+}	0.26	0.18	0.29	0.36	0.26	0.15	0.27	0.37

2.2. ^{1}H NMR spectra of 1AC, 2AC and their complexes with Mg^{2+} and Ca^{2+}

To clarify these changes of the complexes in detail, a ^{1}H NMR study was conducted in the absence and presence of metal ions in acetonitrile-d_3 at 30 °C. Fig. 2 shows ^{1}H NMR spectra of **1AC**, **2AC** and their Ca^{2+} complexes, respectively. Chemical shift change values ($\Delta\delta$ ppm) after the formation of complexes are presented in Table 2. Crown ether moiety peaks in these compounds series showed similar low magnetic field change values upon complexation for each cation. Moreover, when a crown ether moiety and a carbonyl group were bound cooperatively with cation ions, amide proton N*H* shows a low magnetic shift change, resulting in the electronic interaction between Mg^{2+} and the carbonyl group in these compounds. In the Mg^{2+} complex, the chemical shift change of proton N*H* of **2AC** ($\Delta\delta$=0.35) is larger than that of **1AC** ($\Delta\delta$=0.26). This result is ascribed to the fact that the carbonyl groups of **2AC** are bound more tightly with Mg^{2+} than with that of **1AC**. No significant chemical shift change of these anthracene protons was observed before or after complexation with all metal ions, which shows that no interaction existed between anthracene and benzene moieties.

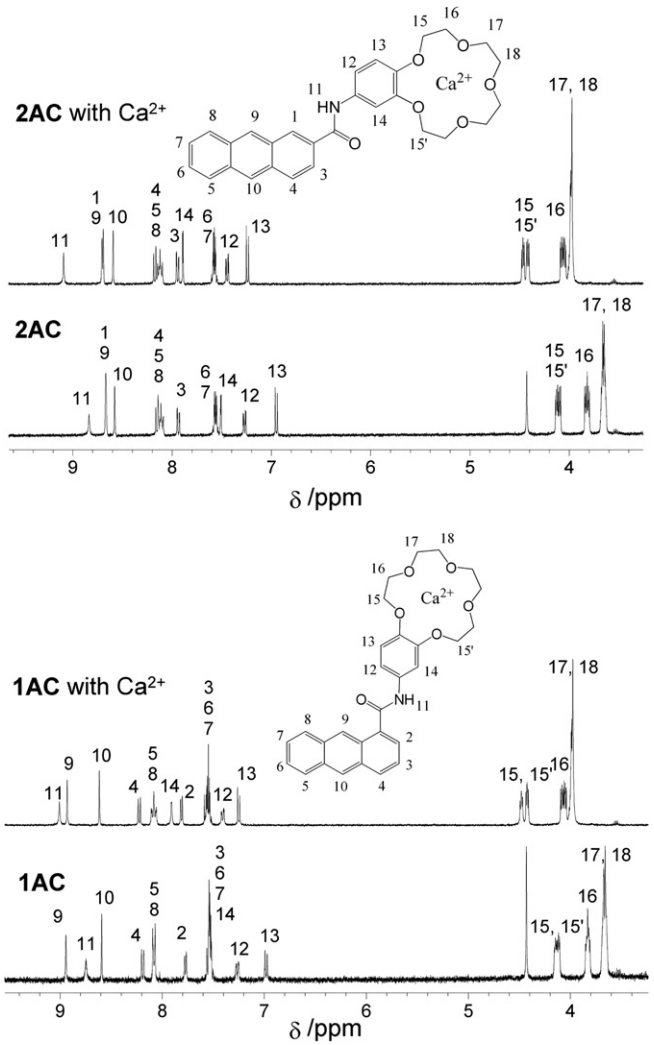

Fig. 2. ^{1}H NMR spectra of **2AC** and **1AC** and their complexes with excess amounts of Ca^{2+} in acetonitrile-d_3 at 30 °C. Peaks on δ=4.41 ppm were impurities in solvent.

2.3. UV absorption spectra of 1AC, 2AC and their complexes with Mg^{2+} and Ca^{2+}

Because ^{1}H NMR study did not afford clear information about the difference of complex structures between **1AC**·Ca^{2+} and **2AC**·Ca^{2+}, complexation behaviors were observed using UV absorption spectroscopy. Fig. 3 depicts UV spectra of (a) **2AC** and its Mg^{2+} complex and (b) **1AC** and its Mg^{2+} complex, respectively. The arrows in the figure indicate directions for the changed spectra with increased concentration of the metal ion. The UV spectra of free **2AC** showed a structureless shape. This phenomenon is expected to be a result of the intramolecular charge transfer from

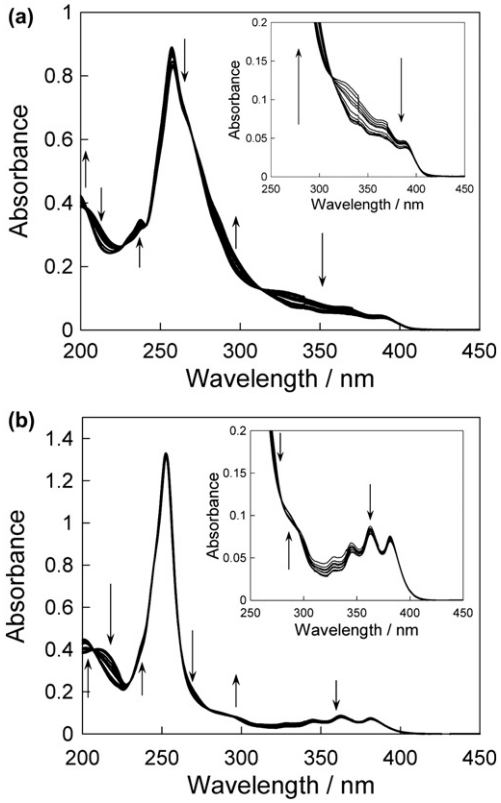

Fig. 3. UV spectra of (a) **2AC** and (b) **1AC** with Mg^{2+} complex in acetonitrile at 25 °C [**L**]=1×10^{-5} mol/dm^3, [Mg^{2+}]=(0, 0.25, 0.5, 0.75, 1, 2, 3, 4, 5, 6)×10^{-5} mol/dm^3.

a carbonyl group to anthracene units of the compound.[15] Upon progressive addition of Mg^{2+}, the absorbance decreased gradually in the region from 312 nm to 395 nm, and increased in the region from 270 nm to 312 nm, as portrayed in the inset of Fig. 3. This result of the latter increase can be attributed to the electronic and steric changes of the π-conjugated system between benzene and the amide bond at the binding event. An isosbestic point at 312 nm was observed, indicating the formation of another species with a different interaction state between anthracene ring and benzene–NH–CO group. In addition, the decrease of absorbance in a region from 241 nm to 270 nm and the increase of absorbance in that from 226 nm to 241 nm with showing an isosbetic point at 241 nm were obtained, which is presumably attributable to the decrease of π-conjugation between NH group and benzene ring. These UV absorption spectral changes were observed in our previous studies.[9] Although UV spectral changes of Mg^{2+} complexes in **1AC** were similar to those of **2AC** in a region from 280 nm to 360 nm, the change in values from 240 nm to 270 nm were small compared with that of **2AC**·Mg^{2+}. Therefore, π-conjugation between NH group and benzene ring did not decrease in the **1AC**·Mg^{2+}. These UV observations strongly suggest that a key step for controlling PET is the breakdown of π-conjugation between the NH group and benzene ring. It became clear that **2AC**, which has a large steric margin, can bend with Mg^{2+} to be interaction by crown ether and carbonyl group. However, **1AC** was unable to accept a deep bending structure at the binding event because of the large steric hindrance between the anthracene ring and crown ether fragment.

2.4. Complex structures of 1AC·Mg^{2+} and 2AC·Mg^{2+}

As our previous data show,[10] rotation of the anthracene ring around the Ph–NH–CO– bond axis in the ground and excited states induces considerable changes in the physical properties of the compound according to their structural positions. Regarding **2AC**, the molecular conformation between 2-anthracene ring and carbonyl group can accommodate a more dramatic steric behavior in electron/charge transfer than either **9AC** or **1AC** for which the carbonyl group remains in nearly similar perpendicular geometry against the anthracene ring.[11b] This geometry change influences the fluorescence nature of anthracene moiety upon complexation. Fluorescence and UV spectral data showed structural and electronic changes of **2AC** upon complexation with metal ions. When a cation was bound by benzo-crown moiety and carbonyl group in **9AC** and **1AC**, the benzo-crown ether moiety and anthracene ring were presumably closer to one another. Strong steric hindrances arose in these structures. To avoid steric crowdedness, deep bending conformation is not acceptable. Such a slight bending conformation did not give the breakdown of π-conjugation between the benzene ring and the NH group for controlling PET relaxation process (Fig. 4). The benzo-crown ether moiety in **2AC** is distant from the anthracene ring, and the space has a large margin. The margin accommodated the **2AC**·Mg^{2+} deep bending conformation, which induced the π-conjugation breakdown (Fig. 4a). The PET relaxation process is not applicable to the excited anthracene unit (Fig. 4b). The fluorescence emission behavior of **2AC** is controllable by the conformational change of the compound upon complexation with cation.

2.5. Cycic voltammetry

To obtain redox potentials, cyclic voltamograms were measured for **9AC**, **1AC**, and **2AC**. Those model compounds were employed for the investigation, which crown or chromophore moieties were displaced by alkyl and alkanoyl amide (*N*-propyl-*x*-anthracenecarboxamide; **xA**, *x*=9, 1, and 2; 4′-butanoylamidobenzo-15-crown-5: **C**). Oxidation and reduction potentials of all compounds were obtained and shown in Table 3. If fluorescence quenching of a chromophore is only driven by the electron donating ability, the tendency of those redox potential accords to those fluorescence enhancement efficiency.[16] Fluorescence quantum yields of this literature were increased with the increasing oxidation potential by modifications of various substituents on the electron donor. However, clear correlation between electronic potentials and fluorescence was not found in Table 3. This result is not enough to explain the difference of fluorescence responses between **2AC** and others from the view of a HOMO–LUMO level of a donor–acceptor. CPK models for **2AC** can be pointed to different directions around amide bond compared with **1AC** and **9AC**. Thus, the result suggests that fluorescence 'off–on' behaviors of present systems is also attributed to steric factor as donor–acceptor arrangement, with the rotation around the amide bond upon the complexation.

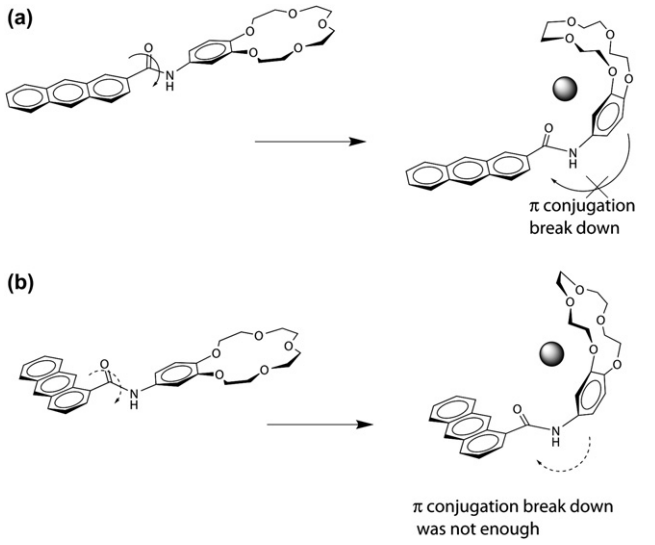

Fig. 4. Schematic representations for complexation of (a) **2AC** and (b) **1AC** with Mg^{2+} and Ca^{2+}.

Table 3
Oxidation and reduction potentials (V) obtained by cyclic voltammetry of crown ethers with Ca^{2+} and those model compounds

	9AC	1AC[a]	2AC[a]	9A	1A	2A	C[b]
Oxidn	1.59	1.57	1.53	1.50	1.49	1.44	1.39
Oxidn	—	1.39	1.33	—	—	—	—
Redn	−1.17	−1.30	−1.02	−1.15	−1.08	−1.00	−1.33

[a] Oxidation and reduction potentials (V) in the absence of Ca^{2+} were also obtained in 0.2 mM solution from the view of solubility: (**1AC**),1.59, 1.30, −0.88; (**2AC**), 1.57, 1.26, −0.82.
[b] Oxidation potentials (V) in the absence of Ca^{2+}: (**C**) 1.23.

3. Conclusion

In summary, we have presented a novel fluorescence sensing mode assisting steric conformations from substitution position on the anthracene ring for detecting cation ions. These chemosensors were synthesized using a simple method of connecting a benzocrown ether and anthracene unit by the amide bond. In these series, their photochemical behaviors showed a fluorescence 'on' state only in 2-anthryl analogue, although 1-anthryl and 9-anthryl analogues displayed non-fluorescence response to cation ions. Results of our study might provide a new protocol for the development of a substitution position effect based fluoroionophore for cation sensing.

4. Experimental

4.1. Syntheses of 4′-(1-anthracene- and 2-anthracenecarboxamido)benzo-15-crown-5 (1AC and 2AC)

1- or 2-Anthracenecarboxylic acid (2.22 g, 0.01 mol) and HOBt (1.53 g, 0.01 mol) were dissolved in 50 mL of DMF; then 4′-aminobenzo-15-crown-5 (5.1 g, 0.018 mol) was added. The solution was treated using dicyclohexylcarbodiimide (3.4 g, 0.018 mol) under stirring for 1 day at 0 °C. The solvent was evaporated under reduced pressure. Thereby, a crude compound was obtained. Compound **1AC** and **2AC** was recrystallized from acetic acid. Model compounds **xA** were also synthesized in the above method from 9-, 1- or 2-anthracenecarboxylic acid (1.11 g, 0.005 mol) and 1-propylamine (0.29 g, 0.005 mol). Compound **C** was prepared as follows: 4′-aminobenzo-15-crown-5 (2.84 g 0.01 mol) and 1-butanoyl chloride (0.53 g, 0.005 mol) dissolved in 50 mL of THF solvent under stirring for 1 day at rt. After filtrated the precipitation, the filtrate was evaporated under reduced pressure. The obtained crude compound was recrystallized from EtOH.

4.2. 4′-(1-Anthracenecarboxamido)benzo-15-crown-5 (1AC)

Yield 65%; pale yellow solid; mp 165–167 °C; ^{1}H NMR (DMSO-d_6, 400 MHz): δ=3.64 (−O−CH_2, m, 8H), 3.80 (−O−CH_2−, m, 4H), 4.07 (−O−CH_2−, m, 4H), 6.97 (aromatic, d, 1H), 7.36 (aromatic, dd, 1H), 7.55 (aromatic, m, 4H), 7.75 (aromatic, d, 1H), 7.76 (aromatic, d, 1H), 8.12 (aromatic, m, 2H), 8.23 (aromatic, d, 1H), 8.29 (aromatic, s, 1H), 8.67 (NH, s, 1H), 8.86 (aromatic, s, 1H); ^{13}C NMR ($SO(CD_3)_2$, 100 MHz): 166.73, 148.42, 144.84, 134.60, 133.31, 131.44, 131.08, 131.04, 130.36, 128.38, 127.73, 127.62, 126.63, 125.94, 125.93, 125.19, 124.21, 124.02, 114.47, 112.37, 106.94, 70.36, 70.33, 69.88, 69.80, 69.04, 68.96, 68.84, 68.52; IR (KBr) ν_{max}: 3292, 2885, 1658, 1229, 1124. Anal. Calcd for $C_{29}H_{29}O_6N$: C, 71.44; H, 6.00; N, 2.87; Found: C, 71.45; H, 5.98; N, 2.88. ESI-MS (m/z) calcd for $C_{29}H_{29}O_6NNa$: 510.19, $[M+Na]^+$; found: 510.19.

4.3. 4′-(2-Anthracenecarboxamido)benzo-15-crown-5 (2AC)

Yield 70%; pale yellow solid; mp 170–172 °C; ^{1}H NMR ($CDCl_3$, 400 MHz): δ=3.78 (−O−CH_2−, m, 8H), 3.93 (−O−CH_2−, m, 4H), 4.20 (−O−CH_2−, m, 4H), 6.90 (aromatic, d, 1H), 7.05 (aromatic, dd, 1H), 7.25 (aromatic, m, 3H), 7.87 (aromatic, m, 2H), 8.05 (aromatic, m, 2H), 8.11 (aromatic, d, 1H), 8.48 (aromatic, s, 1H), 8.56 (aromatic, s, 1H), 8.95 (NH, s, 1H); ^{13}C NMR ($SO(CD_3)_2$, 100 MHz): 165.03, 148.33, 144.85, 133.05, 132.15, 131.75, 131.56, 131.54, 129.96, 128.38, 128.23, 128.20, 128.01, 127.80, 126.36, 125.97, 125.91, 123.66, 114.28, 112.82, 107.32, 70.40, 70.39, 69.89, 69.80, 68.97, 68.84, 68.48; IR (KBr) ν_{max}: 3310, 2873, 1643, 1232, 1145. Anal. Calcd for $C_{29}H_{29}O_6N$: C, 71.44; H, 6.00; N, 2.87; found: C, 71.36; H, 6.01; N, 2.89. ESI-MS (m/z) calcd for $C_{29}H_{29}NO_6Na$: 510.19, $[M+Na]^+$; found: 510.19.

4.4. 4′-(9-Anthracenecarboxamido)benzo-15-crown-5 (9AC)

^{13}C NMR ($SO(CD_3)_2$, 100 MHz): 166.51, 148.62, 145.06, 133.15, 132.83, 130.65, 128.40, 127.45, 127.26, 126.70, 125.61, 124.96, 114.70, 112.21, 106.79, 70.39, 70.35, 69.92, 69.83, 69.13, 68.98, 68.87, 68.59; IR (KBr) ν_{max}: 3271, 2885, 1658, 1229, 1124. ESI-MS (m/z) calcd for $C_{29}H_{29}NO_6Na$: 510.19, $[M+Na]^+$; found: 510.19. Other data were reported in Ref. 9.

4.5. *N*-Propyl-9-anthracenecaroxamide (9A)

Yield 71%; pale yellow solid; ^{1}H NMR ($CDCl_3$, 400 MHz): δ=1.08(−CH_3, t, 3H), 1.78 (−CH_2−, m, 2H), 3.68 (−CH_2−, m, 2H), 6.03 (−CONH−, s, 1H), 7.50 (aromatic, m, 4H), 8.01 (aromatic, d, 2H), 8.08 (aromatic, d, 2H), 8.47 (−CONH−, s, 1H); ^{13}C NMR ($CDCl_3$, 100 MHz): 169.33, 132.10, 131.05, 128.42, 128.05, 127.97, 126.57, 125.40, 125.03, 41.97, 23.12, 11.66; IR (KBr) ν_{max}: 3252, 3060, 1636. ESI-MS (m/z) calcd for $C_{18}H_{17}NONa$: 286.12, $[M+Na]^+$; found: 286.12.

4.6. *N*-Propyl-1-anthracenecarboxamide (1A)

Yield 62%; white solid; ^{1}H NMR ($CDCl_3$, 400 MHz): δ=1.08 (−CH_3, t, 3H), 1.74 (−CH_2−, m, 2H), 3.58 (−CH_2−, m, 2H), 6.08 (−CONH−, s, 1H), 7.42 (aromatic, m, 1H), 7.49 (aromatic, m, 2H), 7.59 (aromatic, d, 1H), 8.02 (aromatic, m, 2H), 8.07 (aromatic, d, 1H), 8.44 (aromatic, s, 1H), 8.93 (aromatic, s, 1H); ^{13}C NMR ($CDCl_3$, 100 MHz): 169.54, 134.81, 132.18, 131.66, 131.56, 130.85, 128.74, 127.98, 127.78, 126.68, 125.92, 125.74, 124.57, 124.40, 123.77, 41.84, 23.11, 11.59; IR (KBr) ν_{max}: 3251, 2956, 1628. ESI-MS (m/z) calcd for $C_{18}H_{17}NONa$: 286.12, $[M+Na]^+$; found: 286.12.

4.7. *N*-Propyl-2-anthracenecarboxamide (2A)

Yield 68%; yellow solid; ^{1}H NMR ($SO(CD_3)_2$, 400 MHz): δ=0.96(−CH_3, t, 3H), 1.61 (−CH_2−, m, 2H), 3.30 (−CH_2−, m, 2H), 7.58 (aromatic, m, 1H), 7.91 (aromatic, dd, 2H), 8.15 (aromatic, m, 3H), 8.63 (aromatic, d, 2H), 8.66 (aromatic, t, 1H), 8.71 (−CONH−, s, 1H); ^{13}C NMR ($SO(CD_3)_2$, 100 MHz): 166.06, 131.98, 131.50, 131.46, 130.48, 130.07, 128.14, 128.03, 127.97, 127.79, 127.58, 126.20, 125.85, 125.79, 123.56, 41.17, 22.49, 11.58; IR (KBr) ν_{max}: 3255, 2959, 1630. ESI-MS (m/z) calcd for $C_{18}H_{17}NONa$: 286.12, $[M+Na]^+$; found: 286.12.

4.8. 4′-Butanoylamidobenzo-15-crown-5 (C)

Yield 67%; pale yellow solid; ^{1}H NMR (CD_3CN, 400 MHz): δ=0.95 (−CH_3, t, 3H), 1.68 (−CH_2−, m, 2H), 2.24 (−CH_2−, t, 2H), 3.62 (−O−CH_2−, m, 8H), 3.77 (−O−CH_2−, m, 4H), 4.02 (−O−CH_2−, m, 4H), 6.82 (aromatic, d, 1H), 6.98 (aromatic, dd, 1H), 7.28 (aromatic, d, 1H), 8.06 (−CONH−, s, 1H); ^{13}C NMR ($CDCl_3$, 100 MHz): 170.83, 149.42, 145.66, 132.21, 114.99, 112.05, 107.05, 71.13, 71.06, 70.69, 70.52, 69.85, 69.75, 69.53, 68.94, 39.66, 19.09, 13.84; IR (KBr) ν_{max}: 3280, 2905, 1632, 1260. ESI-MS (m/z) calcd for $C_{18}H_{27}NO_6Na$: 376.17, $[M+Na]^+$; found: 376.17.

4.9. Measurements

Fluorescence spectra were measured using (RF-5300PC; Shimadzu Corp.) at 25 °C. The excitation wavelength was 363 nm. Concentrations of the fluorescent reagents were 1×10^5 mol/dm^3 in purified acetonitrile. Alkaline earth metal cations were added to the solution of fluorescent reagent as perchlorate salts. The UV spectra were recorded (UV-2400; Shimadzu Corp.) with a device equipped with a temperature controller in spectral grade acetonitrile. Fluorescence quantum yields (Φ_f) were measured for **2AC** and its complex with Ca^{2+}. Aqueous solution containing quinine (0.01 mM) and sulfuric acid (0.05 mM) was used as standard to be Φ_f=0.55 at 25 °C (excitation: 365 nm) in the experiment. ^{1}H and ^{13}C NMR spectra were measured at 30 °C (JNM-EX400; JEOL). For measurements of ^{1}H NMR metal complexes, excess amounts of metal cations as perchlorate salts were added to these solutions. MS were registered on Exactive (Thermo Scientific). IR spectra were obtained by FT/IR-230 (JASCO). Cyclic voltammetry was carried out and three electrodes were selected as bellow: glassy carbon as the working electrode, Ag/AgCl electrode as the reference electrode, Pt wire as the auxiliary electrode. All samples were prepared to 1.0 mM with ca. 5 mM of Ca^{2+} including 0.1 M

tetrabutylammonium perchlorate (TABP) as supporting electrolyte in acetonitrile. Sample solutions were bubbled with nitrogen gas for 5 min before each measurement.

Acknowledgements

The authors are thankful to Prof. S. Tanaka and Mr. Y. Hamade for supporting CV measurement; the authors are also thankful to Assoc. Prof. Y. Kamiya and Mr. Y. Miura for supporting IR measurement (Research Faculty of Environmental Earth Science, Hokkaido Univ.). We would like to thank Ms. S. Oka for MS measurement (Instrumental Analysis Division, Equipment Management Center, Creative Research Institution, Hokkaido Univ.).

References and notes

1. (a) de Silva, A. P.; Gunaratne, H. Q. N.; Gunnlaugsson, T.; Huxley, A. J. M.; McCoy, C. P.; Rademacher, J. T.; Rice, T. E. *Chem. Rev.* **1997**, *97*, 1515; (b) Fabbrizzi, L.; Poggi, A. *Chem. Soc. Rev.* **1995**, *24*, 197; (c) Valeur, B.; Leray, I. *Coord. Chem. Rev.* **2000**, *205*, 3; (d) McQuade, D. T.; Pullen, A. E.; Swager, T. M. *Chem. Rev.* **2000**, *100*, 2537.
2. (a) de Silva, A. P.; Fox, D. B.; Huxley, A. J. M.; Moody, T. S. *Coord. Chem. Rev.* **2000**, *205*, 41; (b) de Silva, A. P.; Gunaratne, H. Q. N.; Gunnlaugsson, T. *Tetrahedron Lett.* **1998**, *39*, 5077; (c) Mineno, T.; Ueno, T.; Urano, Y.; Kojima, H.; Nagano, T. *Org. Lett.* **2006**, *8*, 5963; (d) Matsumoto, T.; Urano, Y.; Shoda, T.; Kojima, H.; Nagano, T. *Org. Lett.* **2007**, *9*, 3375; (e) Ueno, T.; Urano, Y.; Setsukinai, K.; Takakusa, H.; Kojima, H.; Kikuchi, K.; Ohkubo, K.; Fukuzumi, S.; Nagano, T. *J. Am. Chem. Soc.* **2004**, *126*, 14079; (f) Xue, L.; Liu, C.; Jiang, H. *Org. Lett.* **2009**, *11*, 1655; (g) Unob, F.; Asfari, Z.; Vicen, J. *Tetrahedron Lett.* **1998**, *39*, 2951; (h) Kubo, K.; Kato, N.; Sakurai, T. *Bull. Chem. Soc. Jpn.* **1997**, *70*, 3041.
3. (a) Jørgensen, T.; Hansen, T. K.; Becher, J. *Chem. Soc. Rev.* **1994**, *23*, 41; (b) Nielsen, M. B.; Lomholt, C.; Becher, J. *Chem. Soc. Rev.* **2000**, *29*, 153; (c) Ji, Y.; Zhang, R.; Li, Y. J.; Li, Y. Z.; Zuo, J. L.; You, X. Z. *Inorg. Chem.* **2007**, *46*, 866; (d) Liu, W.; Chen, Y.; Wang, R.; Zhou, X. Z.; Zuo, J. L.; You, X. Z. *Organometallics* **2008**, *27*, 2990.
4. (a) de Silva, A. P.; Gunaratne, H. Q. N.; McCoy, C. P. *J. Am. Chem. Soc.* **1997**, *119*, 7891; (b) de Silva, S. A.; Amorelli, B.; Isidor, D. C.; Loo, K. C.; Crooker, K. E.; Pena, Y. E. *Chem. Commun.* **2002**, 1360.
5. (a) Gobbi, L.; Seiler, P.; Diederich, F. *Angew. Chem., Int. Ed.* **1999**, *38*, 674; (b) Beyeler, A.; Belser, P.; De Cola, L. *Angew. Chem., Int. Ed.* **1997**, *36*, 2779.
6. (a) Plush, S. E.; Lincoln, S. F.; Wainwright, K. P. *Inorg. Chim. Acta* **2009**, *362*, 3097; (b) Trupp, S.; Hoffmann, P.; Henke, T.; Mohr, G. J. *Org. Biomol. Chem.* **2008**, *6*, 4319; (c) Cui, D.; Qian, X.; Liu, F. *Org. Lett.* **2004**, *6*, 2757; (d) Niu, C.-G.; Zeng, G.-M.; Chen, L.-X.; Shena, G.-L.; Yu, R.-Q. *Analyst* **2004**, *129*, 20; (e) Michael, K. L.; Taylor, L. G.; Walt, D. R. *Anal. Chem.* **1999**, *71*, 2766; (f) Cajlakovic, M.; Lobnik, A.; Werner, T. *Anal. Chim. Acta* **2002**, *455*, 207; (g) Callan, J. F.; de Silva, A. P.; McClenaghan, N. D. *Chem. Commun.* **2004**, 2048.
7. Uchiyama, S.; Kawai, N.; de Silva, A. P.; Iwai, K. *J. Am. Chem. Soc.* **2004**, *126*, 3032.
8. (a) Fabbrizzi, L.; Licchelli, M.; Mascheroni, S.; Poggi, A.; Sacchi, D.; Zema, M. *Inorg. Chem.* **2002**, *41*, 6129; (b) De Santis, G.; Fabbrizzi, L.; Licchelli, M.; Sardone, N.; Velders, A. H. *Chem.—Eur. J.* **1996**, *2*, 1243; (c) Zhang, G.; Zhang, D.; Guo, X.; Zhu, D. *Org. Lett.* **2004**, *6*, 1209.
9. Kim, J.; Morozumi, T.; Nakamura, H. *Tetrahedron* **2008**, *64*, 10735.
10. Morozumi, T.; Anada, T.; Nakamura, H. *J. Phys. Chem. B* **2001**, *105*, 2923.
11. (a) Kim, J.; Morozumi, T.; Nakamura, H. *Chem. Lett.* **2009**, *38*, 994; (b) Kim, J.; Morozumi, T.; Hiraga, H.; Nakamura, H. *Anal. Sci.* **2009**, *25*, 1319; (c) Kim, J.; Morozumi, T.; Nakamura, H. *Org. Lett.* **2007**, *9*, 4419.
12. Oka, Y.; Nakamura, S.; Morozumi, T.; Nakamura, H. *Talanta* **2010**, *82*, 1622.
13. (a) Hama, H.; Morozumi, T.; Nakamura, H. *Tetrahedron Lett.* **2007**, *48*, 1859; (b) Hama, H.; Morozumi, T.; Nakamura, H. *Anal. Sci.* **2007**, *23*, 1257; (c) Oka, Y.; Hama, H.; Morozumi, T.; Nakamura, H. *Anal. Sci.* **2009**, *25*, 617.
14. Marquardt, D. W. *J. Soc. Ind. Appl. Math.* **1963**, *11*, 431.
15. Werner, T. C.; Hercules, D. M. *J. Phys. Chem.* **1969**, *73*, 2005; Werner, T. C.; Hercules, D. M. *J. Phys. Chem.* **1970**, *74*, 1030.
16. Urano, Y.; Kamiya, M.; Kanda, K.; Ueno, T.; Hirose, K.; Nagano, T. *J. Am. Chem. Soc.* **2005**, *127*, 4888.